Crystallographic and Enzymatic Investigations on the Role of Ser558, His610, and Asn614 in the Catalytic Mechanism of *Azotobacter vinelandii* Dihydrolipoamide Acetyltransferase (E2p)[†,‡]

Jörg Hendle,[§] Andrea Mattevi,[∥,⊥] Adrie H. Westphal,[#] Johan Spee,[#] Arie de Kok,[#] Alex Teplyakov,[○] and Wim G. J. Hol*[,§]

Department of Biological Structure, Biomolecular Structure Program and Howard Hughes Medical Institute, SM-20, University of Washington, Seattle, Washington 98195, Department of Biophysical Chemistry, University of Groningen, 9747 AG Groningen, The Netherlands, Department of Biochemistry, Agricultural University of Wageningen, 6703 HA Wageningen, The Netherlands, and EMBL Outstation, DESY, 22603 Hamburg, Germany

Received September 6, 1994; Revised Manuscript Received December 8, 1994[⊗]

ABSTRACT: Dihydrolipoamide acetyltransferase (E2p) is the structural and catalytic core of the pyruvate dehydrogenase multienzyme complex. In *Azotobacter vinelandii* E2p, residues Ser558, His610′, and Asn614′ are potentially involved in transition state stabilization, proton transfer, and activation of proton transfer, respectively. Three active site mutants, S558A, H610C, and N614D, of the catalytic domain of *A. vinelandii* E2p were prepared by site-directed mutagenesis and enzymatically characterized. The crystal structures of the three mutants have been determined at 2.7, 2.5, and 2.6 Å resolution, respectively. The S558A and H610C mutants exhibit a strongly (200-fold and 500-fold, respectively) reduced enzymatic activity whereas the substitution of Asn614′ by aspartate results in a moderate (9-fold) reduced activity. The decrease in enzymatic activity of the S558A and H610C mutants is solely due to the absence of the hydroxyl and imidazole side chains, respectively, and not due to major conformational rearrangements of the protein. Furthermore the sulfhydryl group of Cys610′ is reoriented, resulting in a completely buried side chain which is quite different from the solvent-exposed imidazole group of His610′ in the wild-type enzyme. The presence of Asn614′ in *A. vinelandii* E2p is exceptional since all other 18 known dihydrolipoamide acyltransferase sequences contain an aspartate in this position. We observe no difference in conformation of Asp614′ in the N614D mutant structure compared with the conformation of Asn614′ in the wild-type enzyme. Detailed analysis of all available structures and sequences suggests two classes of acetyltransferases: one class with a catalytically essential His-Asn pair and one with a His-Asp-Arg triad as present in chloramphenicol acetyltransferase [Leslie, A. G. W. (1990) *J. Mol. Biol. 213*, 167−186] and in the proposed active site models of *Escherichia coli* and yeast E2p.

2-Oxo acid dehydrogenases are a family of very large (5−10 MDa) multienzyme complexes fueling catabolic pathways with CoA-activated acyl groups by catalyzing the irreversible oxidative decarboxylation of 2-oxo acids described by the overall reaction:

$$R{-}CO{-}CO_2^{\ominus} + CoASH + NAD^{\ominus} \rightarrow R{-}CO{-}SCoA + CO_2 + NADH$$

Unraveling the complex reaction mechanism of these complexes at the atomic level is a fascinating subject in biochemistry and structural biology. The pyruvate dehydrogenase complex (PDC)[1] connects glycolysis and the citric acid cycle by converting pyruvate to acetyl-CoA. Further members of this multienzyme family are the 2-oxoglutarate dehydrogenase complex (OGDC) and the branched-chain 2-oxo acid dehydrogenase complex (BCOADC). In various organisms, PDC is composed of multiple copies of at least three enzymes: pyruvate decarboxylase-dehydrogenase (E1p), dihydrolipoamide acetyltransferase (E2p), and dihydrolipoamide dehydrogenase (E3). Dihydrolipoamide acetyltransferase plays a crucial role in the architecture of the complex (Reed, 1974; Perham, 1991; Mattevi et al., 1992b). In the present paper, we address aspects of the catalytic mechanism of E2p.

All dihydrolipoamide acyltransferases possess a unique multidomain structure. The N-terminus of E2p from *Azotobacter vinelandii* and *Escherichia coli* is built up of 3 lipoyl domains of about 80 residues each arranged in a tandem repeat of highly homologous sequences. Each domain

[†] Part of this work was supported by the Netherlands Foundation for Chemical Research (SON) with financial aid from the Netherlands Organization for Scientific Research (NWO). A major equipment grant from the Murdock Charitable Trust for the Biomolecular Structure Center of the School of Medicine of the University of Washington is gratefully acknowledged.

[‡] Atomic coordinates for the S558A, H610C, and N614D mutants of the catalytic domain of *Azotobacter vinelandii* dihydrolipoamide acetyltransferase have been deposited with the Brookhaven Protein Data Bank under Accession Numbers 1DPD, 1DPB, and 1DPC, respectively.

* To whom correspondence should be addressed.

[§] University of Washington.

[∥] University of Groningen.

[⊥] Current address: Department of Genetics and Microbiology, University of Pavia, 27100 Pavia, Italy.

[#] Agricultural University of Wageningen.

[○] EMBL Outstation.

[⊗] Abstract published in *Advance ACS Abstracts,* March 15, 1995.

[1] Abbreviations, E2p, dihydrolipoamide acetyltransferase; E2pCD, catalytic domain of dihydrolipoamide acetyltransferase; PDC, pyruvate dehydrogenase complex; OGDC, 2-oxoglutarate dehydrogenase complex; BCOADC, branched-chain 2-oxo acid dehydrogenase complex; PTA, phosphotransacetylase.

0006-2960/95/0434-4287$09.00/0

contains a lysine residue covalently linked to a lipoic acid molecule, which acts as the coenzyme of the acetyltransferase activity. The N-terminal domains are followed by the E1/E3-binding domain comprising 35−40 residues and the C-terminal catalytic domain consisting of about 250 residues. All domains are connected by long segments comprising 20−40 residues rich in alanine, proline, and/or charged residues providing a high degree of flexibility for the lipoyl domains (Reed & Hackert, 1990; Hanemaaijer et al., 1988; Perham et al., 1981). The total number of residues in *A. vinelandii* E2p is 637.

Several structures of components of the multienzyme complexes have been solved at atomic resolution in recent years. X-ray structures of three dihydrolipoamide dehydrogenases from *A. vinelandii*, *Pseudomonas putida*, and *Pseudomonas fluorescens* confirmed the structural and functional features of E3 as a member of the family of dimeric FAD-dependent disulfide oxidoreductases (Mattevi et al., 1991, 1992a, 1993a). With the NMR structures of the lipoyl domain of *Bacillus stearothermophilus* PDC (Dardel et al., 1991) and the binding domain of *E. coli* OGDC (Robien et al., 1992) together with the X-ray structure of the catalytic domain of *A. vinelandii* PDC (Mattevi et al., 1992b, 1993b), representative structures for each of the three individual domains of the modular and highly flexible E2 polypeptide chain are available. It has been well established that the catalytic domains of E2 are organized as trimers with numerous interactions between the subunits (Mattevi et al., 1992b, 1993b). In *A. vinelandii*, eight trimers are arranged into a hollow truncated cube. The active site is located in the subunit interface, forming a channel with CoA entering from the inside of the hollow cube and acetyl lipoamide entering from the outer surface of the cube (Mattevi et al., 1992b, 1993c).

Comparison of E2 with chloramphenicol acetyltransferase (Guest, 1987), a trimeric enzyme catalyzing a reaction analogous to that of E2, as well as sequence alignment of 13 E2 sequences (Russell & Guest, 1991a), predicted 2 highly conserved residues, a histidine and an aspartic acid, to be involved in the catalytic reaction of E2. An extensive study on X-ray structures derived from binary and tertiary complexes of the catalytic domain of *A. vinelandii* dihydrolipoamide acetyltransferase (E2pCD) with CoA and dihydrolipoamide confirmed the participation of His610′ in catalysis (Mattevi et al., 1993c). His195 is the corresponding residue in the chloramphenicol acetyltransferase structure (Leslie, 1990). The active site Asp199 of chloramphenicol acetyltransferase is structurally equivalent to Asn614′ in the E2 enzyme of *A. vinelandii*. Furthermore, the X-ray structures of binary and tertiary complexes of *A. vinelandii* E2p with substrates, as well as with sulfite, revealed a serine, Ser558, to be involved in catalysis (Mattevi et al., 1993c), which finds its counterpart as Ser148 in the chloramphenicol acetyltransferase structure. The three active site residues, His610′, Asn614′, and Ser558, of *A. vinelandii* E2p are the focus of this paper.

His610′ of *A. vinelandii* E2pCD is a completely conserved residue near the C-terminus of the catalytic domain in 19 known amino acid sequences of dihydrolipoamide acyltransferases (data not shown). His610′ acts as a general base in the catalytic reaction (Figure 1). In a complex of the enzyme with either dihydrolipoamide or CoA, it appears that the Nϵ2 of His610′ forms a hydrogen bond of 3.2 Å to the reactive sulfur atom of dihydrolipoamide (atom S8) and is 4.0 Å apart from the reactive sulfur of CoA (Mattevi et al., 1993c). Mutations of the corresponding histidine residue to cysteine in *E. coli* E2p (Russell & Guest, 1990), and to asparagine and glutamine in bovine E2p (Griffin & Chuang, 1990), resulted in a complete loss of the acyltransferase activity whereas, quite remarkably, the exchange to alanine or asparagine in yeast E2p did not significantly affect the catalytic activity (Niu et al., 1990).

Asn614′ of *A. vinelandii* E2pCD is a remarkable exception from an otherwise completely conserved aspartic acid residue in all known dihydrolipoamide acyltransferases. In the binary complexes of *A. vinelandii* E2pCD with either CoA or hydrogen sulfite, the Oδ1 of Asn614′ provides a hydrogen bond to the Nδ1 of His610′ (Mattevi et al., 1993c), thereby stabilizing the protonated state of the imidazole side chain after the abstraction of the hydrogen from the reactive CoA sulfur (Figure 1). The structural observations and the high enzymatic activity of the asparagine containing *A. vinelandii* enzyme have to be reconciled with mutational studies where the corresponding aspartic acid was replaced by (i) asparagine, alanine, or glutamic acid in yeast E2p (Niu et al., 1990), by (ii) asparagine in *E. coli* E2p (Guest et al., 1990), and by (iii) asparagine or alanine in chloramphenicol acetyltransferase (Lewendon et al., 1988), all of which were accompanied by significantly reduced activity.

Ser558 of *A. vinelandii* E2pCD is another highly conserved residue, which is in 6 out of the 19 known sequences conservatively substituted by threonine and in one case by asparagine. Ser558 is supposed to stabilize the negatively charged tetrahedral intermediate of the acyltransferase reaction (Figure 1) as mimicked in the *A. vinelandii* E2pCD−hydrogen sulfite complex where the Oγ of Ser558 forms a hydrogen bond with a 3.0 Å distance to one of the oxygen atoms of hydrogen sulfite (Mattevi et al., 1993c). The mutation of the corresponding serine to alanine in *E. coli* E2p (Russell & Guest, 1991b) and into alanine, glycine, cysteine, or asparagine in chloramphenicol acetyltransferase (Lewendon et al., 1990) drastically reduced the catalytic activity.

Single-site mutations are a well-known tool for probing functional and structural residues involved in substrate binding and catalysis. In the present paper, the ambiguous role of His610′ in catalysis, the exceptional presence of Asn614′, and the function of Ser558 in *A. vinelandii* dihydrolipamide acetyltransferase are investigated. We describe here the site-directed mutagenesis and overexpression of three single-site mutations H610C, N614D, and S558A, and their catalytic properties together with the crystallization and X-ray structure determination of the mutant proteins.

MATERIALS AND METHODS

Materials. Restriction endonucleases, DNA polymerase I (Klenow fragment), and T4-DNA ligase were purchased from Bethesda Research Laboratories (BRL). Universal M13 sequencing primer, dNTPs, ddNTPs, and calf intestinal phosphatase were obtained from Boehringer. [α-^{32}P]dATP (3000 Ci/mmol) was purchased from New England Nuclear. Superose-12, DEAE-Sepharose, and Sephacryl S-400 were from Pharmacia Fine Chemicals. Oligonucleotides were prepared using a Cyclone DNA synthesizer (Bioresearch Inc.). All other chemicals used were of analytical grade.

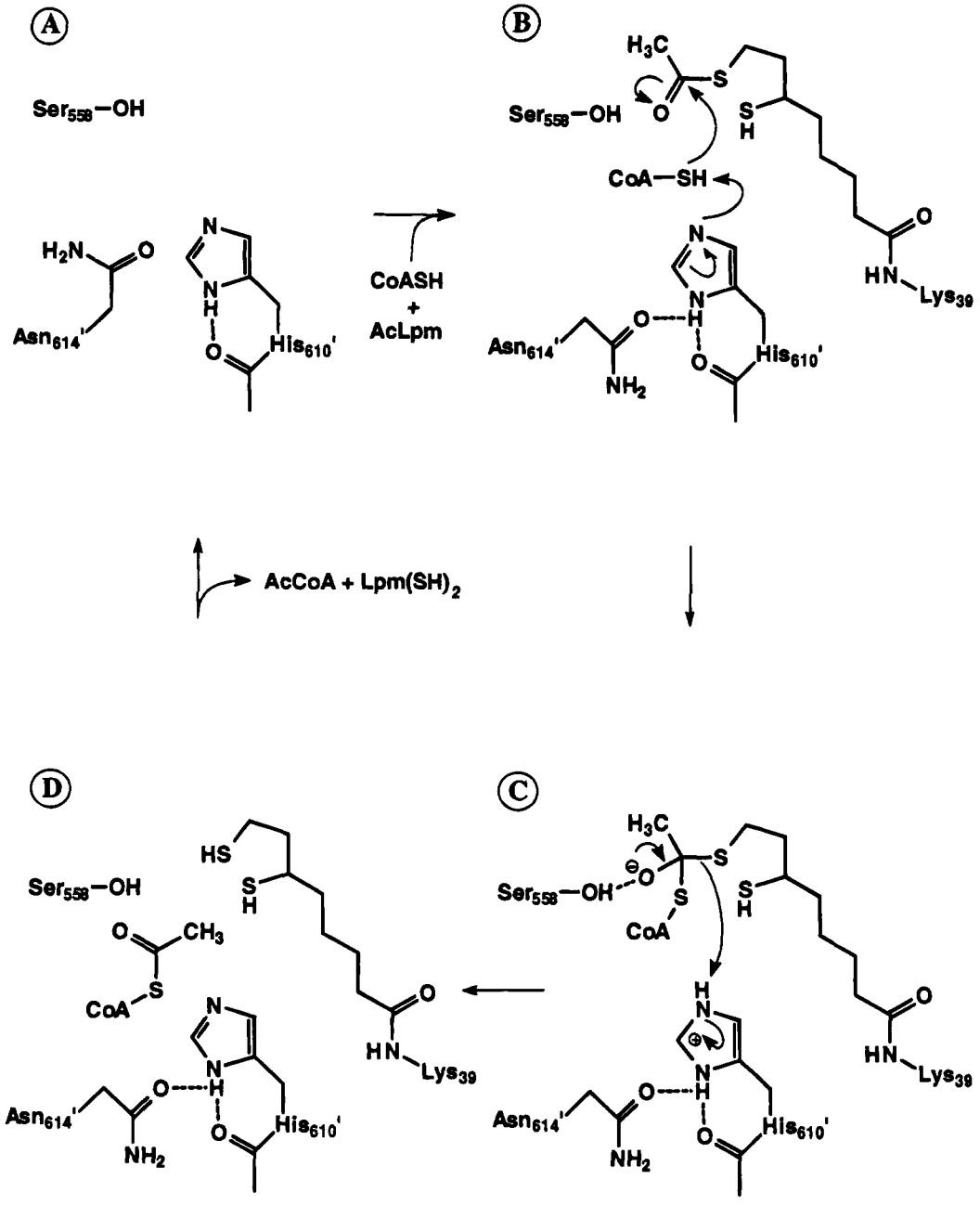

FIGURE 1: Catalytic cycle of the acetyltransferase reaction. Primed residues are provided by another subunit in the E2p trimer than the unprimed residues [see also Mattevi et al. (1992b, 1993c)]. (A) In the ground state, the side chain of Asn614′ is engaged in a hydrogen bond with Asp508 (not shown for simplicity reasons), thereby blocking the CoA-binding channel at the pantetheine moiety of CoA. The unusual side chain conformation of His610′ [see also Mattevi et al. (1992b)] is stabilized by a hydrogen bond between Nδ1 and its own carbonyl O. (B) During binding of reduced CoA (CoASH), a reorientation of the Asn614′ side chain allows the accommodation of the CoA whereby the Asn614′ side chain rotates around the χ_1 torsion angle by about 125° and forms a new hydrogen bond with His610′. The thereby increased nucleophilicity of the His610′ Nε2 atom abstracts the hydrogen atom from the reactive sulfhydryl group of CoA. This sulfur atom subsequently attacks the carbonyl carbon of the acetyl moiety of acetyllipoamide. (C) The resultant tetrahedral intermediate is stabilized by a single hydrogen bond donated from the hydroxyl group of Ser558. The rearrangement of the trigonal planar acetyl carbonyl group results in the simultaneous release of a completely reduced dithiolane group of the lipoamide and acetyl-CoA. (D) The catalytic cycle closes by the release of dihydrolipoamide and acetyl-CoA from the active site. Departure of acetyl-CoA causes a rotation of the Asn614′ side chain back into the position of the ground state.

Bacterial Strains and Vectors. *E. coli* strain TG2, a *recA*$^-$ version of TG1, i.e., Δ(*lac-pro*), *thi*, *supE*, [Res$^-$ Mod$^-$ (k)], F′ (*tra*D36 *pro* A$^+$ B$^+$, *laqI*^{q} Z ΔM15), was used throughout (Gibson, 1984). The phages M13mp18 and M13mp19 were used for sequencing according to the dideoxy chain termination method of Sanger (Sanger et al., 1977). *E. coli* strain RZ1032 [*SupE*, *duf*, *ung*$^-$] was used for site-directed mutagenesis (Kunkel et al., 1987). Standard DNA operations were performed as described in Ausbel et al. (1987).

Construction of Plasmids. For the construction of plasmids containing the desired mutations, the plasmid pACAT2 (encoding the *A. vinelandii* E2p catalytic domain) (Schulze et al., 1991a) was used as a starting material. From this plasmid, a 551 bp *Sph*I–*Xba*I fragment containing the mutation region for His610′ and Asn614′ and a 750 bp *Sph*I–*Sph*I fragment for the Ser558 mutation region were ligated into M13mp18. Site-directed mutagenesis was carried out according to the method of Kunkel (Kunkel et al., 1987)

Table 1: Data Collection and Refinement Statistics for the E2pCD Mutants S558A, H610C, and N614D

protein	E2pCD S558A	E2pCD H610C	E2pCD N614D
resolution (Å)	10.0−2.7	10.0−2.5	10.0−2.6
cell axis (Å)	224.6	225.0	224.9
no. of observations	191748	52974	36952
no. of unique reflections[a]	13826	13426	13594
completeness (%)	99.8	78.7	93.3
R_{sym}[b] (%)	10.8	7.1	7.2
R-factor[b] (%)	18.4	18.7	18.4
no. of solvents	51	40	38
rms bonds[c] (Å)	0.014	0.013	0.012
rms angles[c] (deg)	3.0	2.9	2.9
rms coordinates[d] (Å)	0.17	0.15	0.15
mean *B*-value main chain (Å^2)	16.6	17.4	29.7
mean *B*-value solvent (Å^2)	29.2	29.9	43.3

[a] All reflections with $I/\sigma > 1.0$. [b] The R_{sym} is defined as $R_{sym} = \Sigma|I - \langle I\rangle|/\Sigma\langle I\rangle$ and the crystallographic *R*-factor as $R = \Sigma|F_{calc} - F_{obs}|/\Sigma F_{obs}$. [c] The rms deviations from the ideal bond lengths and angles were calculated with XPLOR (Brünger et al., 1990). [d] The rms deviation of the main chain atoms between the mutant protein and the wild type (Mattevi et al., 1992b).

with modifications described in Schulze et al. (1991b). Next, the mutated fragments were isolated from M13mp18 and ligated into the large *Sph*I−*Sph*I or *Sph*I−*Xba*I plasmid fragment containing the other part of the gene. After transformation of *E. coli* TG2, plasmids pACDS558A, pACDH610C, and pACDN614D were obtained and used for expression of mutated proteins.

Enzyme Isolation and Assay. The catalytic domain from *A. vinelandii* containing the mutations S558A, H610C, and N614D, respectively, was isolated from *E. coli* TG2 according to Schulze et al. (1991a). The purification was monitored by SDS−PAGE. Acetyltransferase activity was determined spectrophotometrically at 240 nm in a coupled assay with phosphotransacetylase (PTA) as described in Bresters et al. (1975). Dihydrolipoamide was prepared by the method of Reed (Reed et al., 1958).

Kinetic Properties of Catalytic Domain Mutants. The K_M and V_{max} values of wild-type catalytic domain and mutants were investigated using the assay described above. Dihydrolipoamide concentrations ranged from 0.1 to 10 mM, and CoA concentrations used were from 1 to 100 mM. The amount of acetyl-CoA produced in the PTA reaction was calculated from the absorption increase at 240 nm, using $\epsilon_{AcCoA} = 3500\ M^{-1}\ cm^{-1}$. The acetyltransferase reaction was then started by the addition of the catalytic domain preparation. The K_M values for dihydrolipoamide and acetyl-CoA were obtained from double-reciprocal plots and subsequent extrapolation to infinite concentration of the other substrate. V_{max} values were obtained by extrapolation to infinite concentration of both substrates. The influence of the pH was studied between pH 6.0 and pH 8.4 in 50 mM Bes buffer. Under the conditions used, the PTA reaction was not rate-limiting.

Crystallization. Crystallization of the mutants S558A, H610C, and N614D of E2pCD was carried out by the vapor diffusion technique at room temperature. Hanging drops of 5 μL of protein (10 mg/mL) in 50 mM HEPES, 0.02% azide, pH 7.0, were mixed with equal volumes of 12−16% ammonium sulfate equilibrated against 12−16% ammonium sulfate in the same buffer. Crystals of S558A and N614D protein appeared within a week and grew up to 0.8 mm × 0.8 mm × 0.8 mm. The size of the small crystals of the H610C mutant (0.2 mm × 0.2 mm 0.2 mm) could be increased by the macroseeding technique (Thaller et al., 1981). It is intriguing that a mutation in the center of the active site channel, far away from any crystal contact, would affect crystal growth.

All three mutants crystallized isomorphously to the wild-type protein (Mattevi et al., 1993b) in the cubic space group *F432* with a cell axis of 224.8 Å. The crystals contain one subunit per asymmetric unit and have an unusually high solvent content of 73%.

Data Collection and Processing. The data set for the S558A crystal was collected on a Fuji image plate of the X-31 synchrotron beam line at the EMBL Outstation Hamburg, Germany, using a wavelength of 1.008 Å. Data were recorded with an oscillation range of 0.75° and a crystal-to-detector distance of 270 mm. The data were processed using a version of the MOSCO program package (Machin et al., 1983) modified for image plates, and the CCP4 program suite (1986).

Diffraction data for the H610C crystal were collected on a Siemens X100 area detector using graphite monochromatized CuK_α radiation generated by a Rigaku RU-200 rotating anode operated at 50 kV and 100 mA. The crystal-to-detector distance was set to 210 mm using an oscillation range of 0.25°. The data were processed with the XENGEN program (Howard et al., 1987).

Data collection for the N614D crystal was performed on a R-axis II Imaging Plate System using a Rigaku RU-300 rotating anode run at 60 kV and 300 mA. Data were recorded with an oscillation range of 1.0° and a crystal-to-detector distance of 107 mm using graphite monochromatized CuK_α radiation. The data were processed with the MSC software (Sato et al., 1992).

Statistics for all data sets are given in Table 1. The three data sets are 99.8, 78.7, and 93.3% complete out to a resolution of 2.7, 2.5, and 2.6 Å for the S558A, H610C, and N614D variants, respectively.

Refinement. The crystals of all three mutants were isomorphous with those of the wild-type protein, so the wild-type structure was used as a model for difference Fourier calculations. The initial σ_A weighted (Read, 1986) ($F_{obs}^{mut} - F_{calc}^{wt}$) omit maps calculated with the wild-type phases revealed changes in side chain densities for Cys610′ and Ala558 and, furthermore, a new conformation for the side chain of residue 610′ not seen before in structures of the catalytic domain (Mattevi et al., 1993b,c). For the calculation of the initial omit maps, all atoms of the wild-type model within a sphere of 6 Å around the mutated residue were

Table 2: Kinetic Constants of Wild-Type and Mutant E2pCD[a]

enzyme	k_{cat} (s^{-1})	K_m Lip(SH_2) (mM)	K_m acetyl-CoA (μM)	k_{cat}/K_m ($\times 10^3$ s^{-1} M^{-1}) Lip-($SH)_2$	k_{cat}/K_m ($\times 10^3$ s^{-1} M^{-1}) acetyl-CoA
wild type	144	5.37	22	26.8	6600
S558A	0.86	6.40	28	0.134	30.7
H610C	0.25	5.30	36	0.047	6.9
N614D	16.9	1.08	52	15.6	325

[a] Wild-type and mutant protein: residues 395−637.

omitted, resulting in a loss of approximately 6% of the scattering atoms.

For all three mutants, the initial model, consisting of 243 residues with the mutated residue changed to alanine and no water molecules, was refined with XPLOR (Brünger et al., 1990). The starting *R*-values for all data included in the refinement (Table 1) were 22.8%, 23.4%, and 23.8% for S558A, H610C, and N614D, respectively. The refinement was performed by several cycles of conjugate gradient minimization followed by individual atomic *B*-factor refinement. The resulting models and maps were inspected on Silicon Graphics Workstations with Program-O (Jones et al., 1991). Side chain orientations were adjusted and water molecules were built into density according to 3σ peaks of the $(F_o - F_c)$ maps. Water molecules were checked for proper hydrogen bond interaction. If, upon subsequent refinement, the *B*-factor of a water molecule exceeded 50 Å^2, the molecule was removed from the model.

RESULTS

Expression and Purification of Catalytic Domain Mutants from A. vinelandii. Different mutants (S558A, H610C, and N614D) of the catalytic domain of the acetyltransferase component (E2p) of the pyruvate dehydrogenase complex from *A. vinelandii* were constructed by site-directed mutagenesis. The expression of the mutant proteins in *E. coli* TG2 was very high and reached 20% of the total protein in cell-free extract. For each mutant, about 150 mg of pure protein could be isolated from a 6 L culture after purification.

Kinetic Properties of Catalytic Domain Mutants. K_M and k_{cat} values are summarized in Table 2. The results of the measurements leave no doubt about the function of His610′ or Ser558 in the E2p of *A. vinelandii*. The k_{cat} was reduced to only 0.17% for H610C and 0.6% for S558A to that of the wild-type protein, whereas the K_M values of CoA and dihydrolipoamide have not changed significantly. The N614D mutant behaves clearly different. The enzyme is still quite active with a specific activity of 58% and 5% for dihydrolipoamide and CoA, respectively. The mutation affects the k_{cat}, which is reduced to 12% compared with the wild type, as well as the K_M values. The K_M for dihydrolipoamide is 5-fold decreased, a remarkable improved binding of this substrate which partially compensates the reduced k_{cat}, whereas the K_M for CoA is 2.5-fold increased.

The effect of pH was studied between pH 6.0 and 8.4, a pH range where the enzyme was stable during the time of the measurements. In the activity versus pH plot of wild-type enzyme, a p*K* was observed at pH 6.7. This p*K* did not change in the H610C mutant and is therefore not due to ionization of His610′. More detailed studies are required to analyze the origin of this p*K* value.

At some pH values within this pH range, the activities were measured in Bes, Tris, and potassium phosphate buffers at concentrations from 1 to 120 mM. No significant differences were observed, neither with the wild-type enzyme nor with the mutants. The addition of 10−500 mM NH_4Cl or imidazole had no effect on the activity of the proteins.

Quality of the X-ray Models. The final $(2F_o - F_c)$ maps for all 3 mutants show continuous density for all 243 residues of the catalytic domain, which comprises C-terminal residues 395−637. The three mutant models have crystallographic *R*-factors between 18.4 and 18.7% for all reflections with $I/\sigma > 1.0$ within the given resolution range and good geometry (Table 1). All non-glycine residues, except Ala567 in the N614D structure, Ala567 and Ser583 in the S558A structure, are located in the energetically preferred $\varphi-\psi$ combinations of a Ramachandran plot (Ramachandran et al., 1966). Both Ala567 and Ser583 are within 15° of the allowed regions and coincide with the two outliers of the wild-type structure (Mattevi et al., 1993b).

The rms differences of main chain and side chain atoms between the wild type and the mutant protein are in agreement with the coordinate error estimated by Luzzati plots. The overall rms deviations for all protein atoms compared with the wild-type enzyme are 0.21, 0.19, and 0.27 Å for the S558A, H610C, and N614D mutants, respectively.

The distribution of temperature factors along the protein chain follows for all three mutants the pattern observed for the wild-type protein (Mattevi et al., 1993b) with a slightly decreased average *B*-value for the main chain atoms of the S558A and H610C model of 4.0 and 3.2 Å^2, respectively. The uniformly higher average *B*-value for the main chain atoms of the N614D model of 9.1 Å^2 is most likely due to a higher degree of general disorder in the crystal and appears not to be due to specific flexible parts of the protein.

Wild-Type Structure versus Mutant Structures. The structures of all three variants display no unexpected deviations from the wild-type molecule. The few residues in the variant structures which have rms deviations above 0.6 Å compared with the wild type are located either at the protein surface or in the close vicinity of the mutation site, and the deviations are restricted to side chains only.

The new side chain orientations of Ser440, Lys479, and Glu551 in the S558A mutant allow those residues, located at the protein surface, to form hydrogen bonds not existing in the wild-type protein: Ser 440 Oγ−Sol718 O, 2.8 Å; Lys479 Nζ−Asp522 Oδ1, 2.9 Å; Glu551 Oε1−Tyr406′ OH, 3.1 Å. In the H610C mutant, the reorientation of the Met550 side chain allows this surface residue to form an additional hydrogen bond of 3.4 Å, with the Sδ atom as a potential hydrogen bond acceptor and a solvent molecule as a hydrogen bond donor. This unusual type of hydrogen bond has previous been described in a survey of 85 high-resolution protein structures (Gregoret et al., 1991) where 25% of the screened methionine Sδ atoms were within 4.0 Å of a hydroxyl oxygen or an amino or amide nitrogen. However, in our H610C mutant, this hydrogen bond is not very well-defined due to the high *B*-factor of Met550 Sδ of 48.8 Å^2, while the solvent molecule has a *B*-factor of 34.0 Å^2. The surface residue Ser440 of the N614D mutant presents again a side chain orientation involved in a new hydrogen bond identical to the one between Ser440 and Sol718 of the S558A mutant, whereas the new side chain orientations of the surface residues Glu411 and Glu445 are only weakly defined

Table 3: Averaged Main Chain and Side Chain *B*-Factors from Selected Residues

	averaged *B*-factor (Å^2)							
	wild type		S558A		H610C		N614D	
residue	main	side	main	side	main	side	main	side
Asp508	42.0	47.6	35.2	39.7	42.7	54.0	58.1	76.5
558	12.4	17.3	4.1	2.0	5.7	9.7	16.2	20.9
610′	12.9	12.3	7.1	9.0	14.1	15.6	19.3	23.1
614′	13.8	27.2	8.8	21.6	11.7	24.1	22.1	50.1
all residues	20.6	23.7	16.6	19.7	17.4	20.0	29.7	35.5

by electron density with average *B*-factors for all side chain atoms of 72.0 and 58.4 Å^2, respectively.

The absence of the hydroxyl group of residue 558 in the S558A variant did not induce any significant conformational shifts within the active site (Figure 2a).

The side chain orientation of Cys610′ in the H610C variant represents the most unexpected feature of this variant (Figure 2b). The side chains of Cys610′ in the H610C variant (χ_1, 55°) and of His610′ in the wild-type protein (χ_1, −156°) are pointing in nearly opposite directions. As a result of this change of χ_1 by about 149°, 87% of the solvent-accessible surface (28.8 Å^2 out of 33.2 Å^2) of the sulfhydryl group of Cys610′ is buried. In contrast, the imidazole ring of His610′ in the wild-type enzyme is exposed to the active site solvent molecules with only 30% of the solvent-accessible surface (17.3 Å^2 out of 57.8 Å^2) buried. In the wild-type structure (Mattevi et al., 1992b), as well as in the structures of the S558A and the N614D mutants, the His610′ side chain orientation is fixed by a hydrogen bond between Nδ1 and its own carbonyl O whereas the orientation of the Cys610′ side chain allows a well-defined hydrogen bond between Cys610′ Sγ and Pro433′ O of 3.1 Å.

The side chain of the mutated residue Asp614′, with a (χ_1,χ_2) combination of (62°,−97°), shows virtually the same conformation (Figure 2c) as the side chain of Asn614′ in the wild-type enzyme which has (χ_1,χ_2) values of (49°,−52°). The similar side chain orientations with a local rms difference of only 0.49 Å between them are surprising. In the wild-type enzyme, Asn614′ is located at the subunit interface engaged in a subunit−subunit hydrogen bond between Asp508 Oδ2 and Asn614′ Nδ2 of 3.1 Å. The distance between the corresponding atoms in the N614D variant, Asp508 Oδ2 and Asp614′ Oδ2, is 3.3 Å, a relatively short contact between two aspartic acid side chains. However, the high average *B*-value of 76.5 and 50.1 Å^2 for the side chain atoms of Asp508 and Asp614′, respectively, in the N614D mutant may indicate a local disorder in the Asp−Asp contact, not unexpected for a close contact between two potentially negatively charged residues. It might well be possible that the high *B*-values should be interpreted as an indication of an arrangement in which both side chains occupy the observed conformer only part of the time and never, or quite rarely, at the same time.

The average *B*-values of the main chain atoms for crucial residues in the four E2p structures under consideration are presented in Table 3. The active site residues 558 and 610′ are part of the most rigid residues in the wild type as well as in the three mutant proteins as indicated by their relatively low *B*-values when compared with the average *B*-value of the entire protein. Neither the removal of a hydroxyl group in the S558A variant nor the replacement of the imidazole group by a sulfhydryl group in the H610C variant has altered the mobility of the affected atoms significantly.

DISCUSSION

The enzymological studies and crystal structure determination of three active site mutants improve our understanding of the role of the substituted residues on catalysis. All three mutant structures have been solved in a similar resolution range as the wild-type protein, allowing us to compare structures with the same degree of accuracy. All three mutant proteins crystallized isomorphously without major conformational changes. Consequently, the reduction in catalytic efficiency is due to the changes in side chains.

Ser558 and Stabilization of the Transition State. The S588A variant lacks a hydroxyl group compared to the wild-type protein. In the latter case, Ser558 is involved in binding one of the substrates, coenzyme A, and in stabilizing the hypothetical tetrahedral intermediate (Mattevi et al., 1993c). These two functions are clearly reflected by the kinetic properties of the S558A mutant. The unchanged K_M value for CoA indicates that the binding of CoA to the S558A mutant is not significantly affected by the absence of the single hydrogen bond formed in the wild-type enzyme between Ser558 and the pantetheine moiety of CoA. The second proposed function of Ser558, the stabilization of the transition state, is much more affected by the missing hydrogen bond between Ala558 and the hypothetical tetrahedral intermediate as demonstrated by the more than 2 orders of magnitude reduction of the k_{cat} value for the S558A mutant. Analogous to the enzyme from *E. coli* (Russell & Guest, 1990) and chloramphenicol acetyltransferase (Lewendon et al., 1990), the substitution of the active site serine by alanine drastically reduces the specific activity. Ser558 in *A. vinelandii* E2p and the corresponding serine in *E. coli* E2p as well as in chloramphenicol acetyltransferase are key residues for the enzymatic activity.

Neither the conformation of the main chain and the side chains nor the *B*-factors of the residues in the vicinity of the mutation site S558A are affected by the mutation. The only significant difference between the wild type and the S558A variant is the increased space in the active site of the S558A variant which seems to enable the protein to bind two well-defined solvent molecules more than the active site of the Ser558-containing proteins. All six solvents are connected by hydrogen bonds with each other, building a solvent network shaped like a five-membered ring (Figure 3a). This "ring of solvents" engages at its periphery all active site residues, either involved in catalysis or involved in substrate binding, in hydrogen bonds. Although none of the solvent molecules of the active site is within a distance of 4.0 Å to the Cβ of Ala558, two additional solvents, SolCoA3 and SolLpm3, seem to fill the gap created by removing the hydroxyl group of the wild-type Ser558.

His610′ and General Base Catalysis. The H610C mutant lacks an imidazole group pointing into the active site. This imidazole is involved in binding both substrates, dihydrolipoamide and coenzyme A, and furthermore acts as a general base catalyst (Mattevi et al., 1993c). The kinetic properties of the H610C mutant are very similar to those of the S558A mutant. The K_M values for dihydrolipoamide and CoA are nearly the same as those derived from the wild-type protein whereas the k_{cat} is reduced by almost 3 orders of magnitude.

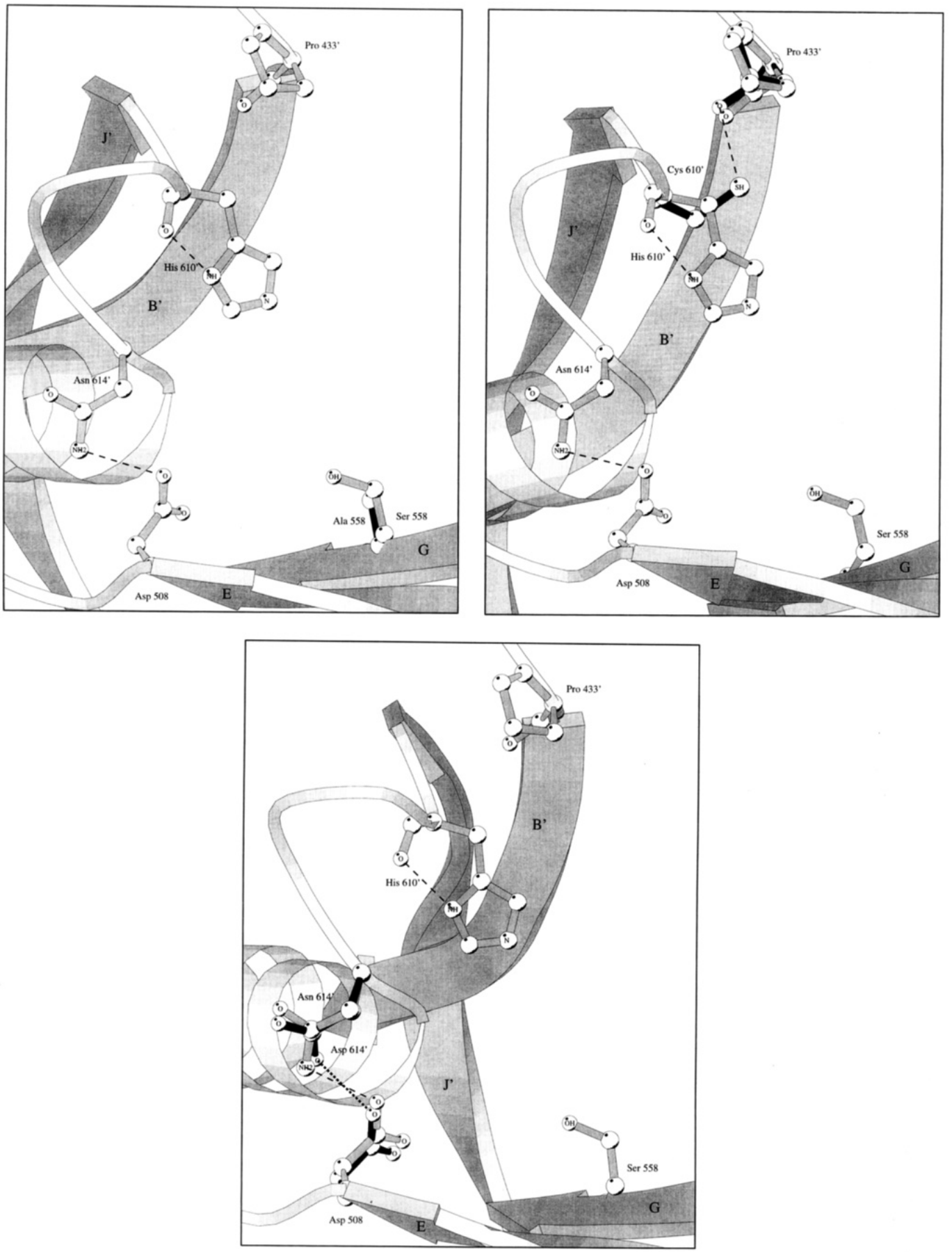

FIGURE 2: Superposition of the active site of the wild-type and (a, top left panel) S558A, (b, top right panel) H610C, and (c, bottom panel) N614D structures. The figures were prepared with Molscript (Kraulis, 1991), representing the wild-type structure in gray shades and parts of the mutant structure which deviate from that of the wild type in solid black. Hydrogen bonds are indicated by dashed lines and contact distances by dotted lines.

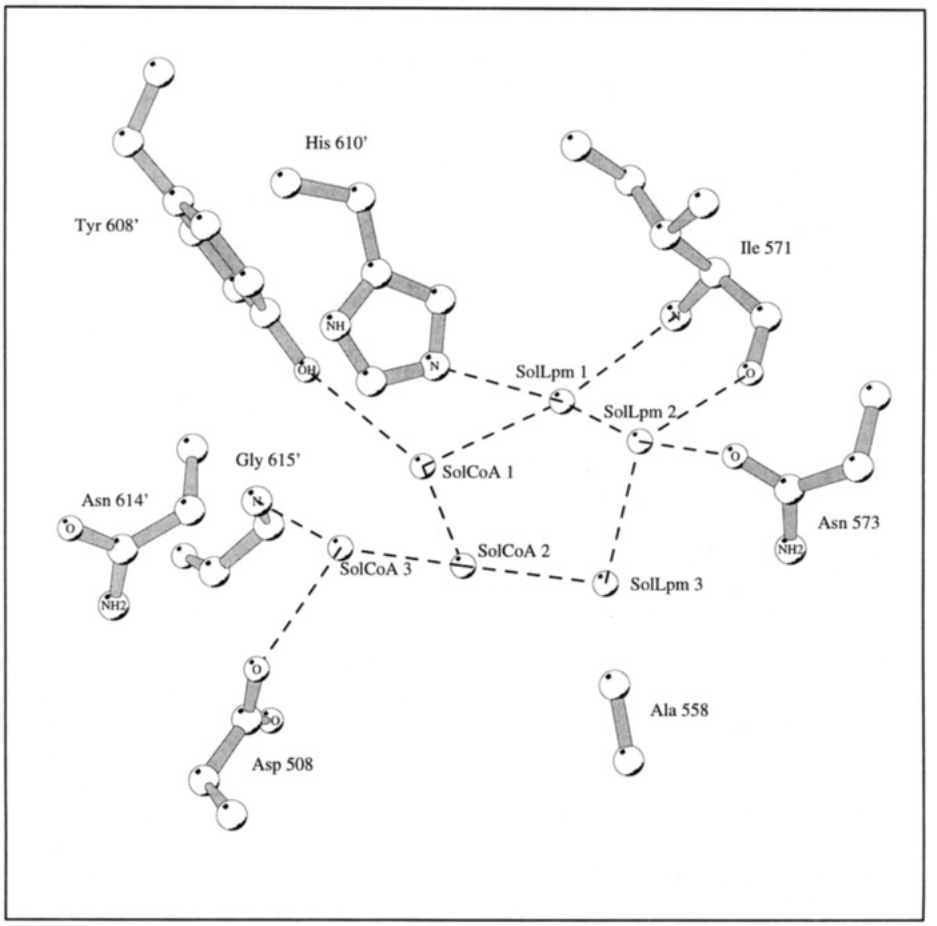

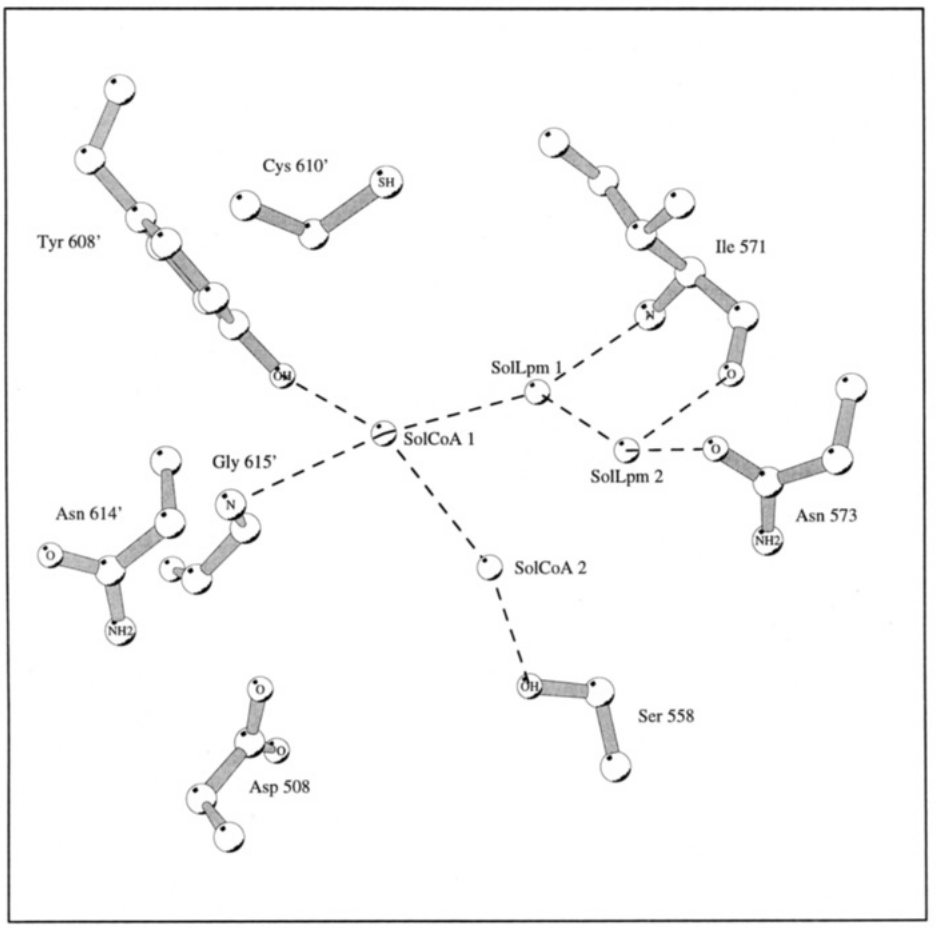

FIGURE 3: Solvent network in the active site of the (a, top panel) S558A and (b, bottom panel) H610C structures. The schemes were prepared with Molscript (Kraulis, 1991) using dashed lines for the presentation of hydrogen bonds.

Therefore, it can be concluded that His610′ does not contribute significantly to the binding of CoA or dihydrolipoamide but it is essential for the catalytic reaction. Our results are in agreement with those of Russell and Guest (1990) and Griffin and Chuang (1990). Like in the *E. coli* or bovine enzyme, the E2p from *A. vinelandii* contains a histidine in the active site whose substitution by cysteine, asparagine, or glutamine results in drastically reduced catalytic activity. In the yeast enzyme, replacement of the corresponding His427 by asparagine or alanine did not significantly affect the K_m or k_{cat} values (Niu et al., 1990). However, it should be pointed out that the yeast E2p is not a very efficient enzyme compared with the *A. vinelandii* E2p, with k_{cat}/K_m for acetyl-CoA 2 orders of magnitude lower than for the *A. vinelandii* enzyme. The k_{cat}/K_m value for the *A. vinelandii* H610C mutant (Table 2) is only 7-fold lower than that of wild-type yeast enzyme (Niu et al., 1990).

In the H610C *A. vinelandii* E2p mutant, the side chain of Cys610′ adopts an unexpected conformation resulting in a buried sulfhydryl group. This conformation might release some strain induced by the unusual side chain conformation of His610′ in the wild-type protein (Mattevi et al., 1992a). Biochemical evidence, such as the lack of reaction between the sulfhydryl group of Cys610′ with sulfhydryl reagents [e.g., *N*-ethylmaleimide, iodoacetic acid, or its fluorescent analogue IAANS (data not shown)], is in agreement with our structural studies. Although the larger reagents may not be able to reach the center of the channel, there is little doubt that iodoacetic acid would be able to do so. The buried sulfhydryl group of Cys610′ replaces neither structurally nor functionally the imidazole group of His610′, which rationalizes the lack of activity of the H610C mutant. However, the residual activity is significant. This might be the result of (i) a Cys610′ side chain conformation occurring during catalysis which deviates from the one observed in the unliganded form discussed in this paper followed by an involvement, in an unknown manner, of the cysteine in catalysis or (ii) a water molecule occupying approximately the former position of the Nε2 atom of the His610′ imidazole ring and acting as a general base catalyst. However, at that position no well-defined electron density representing a water molecule is visible in the $(2F_o - F_c)$ map of the H610C mutant structure (Figure 3b), but this does not rule out a catalytic water being present perhaps only transiently when substrates are bound.

Asn614′ and Activation of His610′. In the N614D mutant, the uncharged side chain of the wild-type enzyme is replaced by a negatively charged carboxylate group. In the unliganded wild-type enzyme, the side chain of Asn614′ adopts a conformation in which a hydrogen bond is formed with the side chain of Asp508. An identical interaction is observed in the H610C and S558A mutants. In the N614D mutant, the new side chain of Asp614′ is adopting a quite similar conformation. A key point is that in this conformation no side chain atom of Asn/Asp614′ is closer than 6.1 Å away from the catalytic residues His610′ or Ser558. This position of the side chain of residue 614′ makes it hard to understand why mutation of this residue would have an effect on the catalytic activity of the enzyme.

However, in the structures of the binary complexes of the wild-type protein with either CoA or hydrogen sulfite, a second conformation of the side chain of Asn614′ is observed (Mattevi et al., 1993c) (Figure 2c and 4a). A possible reason for this conformational change is the fact that the side chain of Asp508 would be too close to the O5P atom of the bound CoA if it remained in the "unliganded" conformation. In the binary complex of E2p with CoA, the side chain of Asp508 is rotated by approximately 101° around its Cα−Cβ bond. As a consequence, Asn614′ is no longer engaged in the hydrogen bond with Asp508, which stabilizes the side chain of Asn614′ in its "unliganded" conformation. In the "liganded" conformation of Asn614′, its side chain is rotated by approximately 124° around its Cα−Cβ bond, and now the Oδ1 of Asn614′ is forming a hydrogen bond, albeit a long one of about 3.4 Å, with the Nδ1 atom of His610′. It is likely that the presence of the amide group of Asn614′ near His610′ enhances the nucleophilicity of the imidazole group and improves its ability to abstract a proton from one incoming sulfhydryl group and release the proton to the sulfhydryl group of the other substrate in the catalytic cycle (see also Figure 1). In the N614D mutant, a carboxylate moiety at the same position is likely to enhance the nucleophilicity of the imidazole group more than a carboxyamide function, and one might have expected that this would improve the catalytic efficiency of the N614D mutant compared with the *A. vinelandii* wild-type enzyme.

The results of our kinetic studies indicate otherwise, however. The k_{cat} of the N614D enzyme is diminished by almost 1 order of magnitude compared to the wild-type enzyme, whereas the K_M for dihydrolipoamide is significantly decreased and the K_M for CoA slightly increased. The 5-fold decreased K_M value for dihydrolipoamide is a surprising result since the binding site for dihydrolipoamide is on the opposite site of the active site channel with respect to the Asp614′ side chain. Overall, the *A. vinelandii* N614D mutant is catalytically less efficient than the wild-type enzyme.

This decreased activity after replacing an amide by a carboxylate function in the side chain of residue 614′ is quite in contrast with the fact, pointed out in the introduction, that *A. vinelandii* is the only enzyme which has an uncharged asparagine residue at position 614′. All 18 other dihydrolipoamide acyltransferases sequenced so far have a charged aspartate at this position, and while the yeast enzyme is less efficient than the *A. vinelandii* enzyme, *E. coli* E2p is as efficient as the *A. vinelandii* E2p, proving that enzymes with an aspartate or an asparagine at position 614′ can be equally efficient.

It is quite intriguing that the N→D substitution has similar effects on the properties of the *A. vinelandii* enzyme as the D→N substitution on the yeast and *E. coli* enzymes (Niu et al., 1990; Guest et al., 1990): the activity decreases in all three cases by approximately 1 order of magnitude. In the case of chloramphenicol acetyltransferase, the corresponding mutation of Asp199 to asparagine also resulted in a loss of activity, but in this case the reduction was approximately a factor of 2000 (Lewendon et al., 1988).

Modulation of the Activator Residue 614′. In the "liganded" conformation of Asn614′ in wild-type *A. vinelandii* E2p, the side chain of Asn614′ essentially only interacts with the catalytic residue His610′ (Figure 4a). The single other interaction of the Asn614′ side chain is between Asn614′ Nδ2 and Met418 Sδ with a distance of 4.0 Å. In chloramphenicol acetyltransferase, however, the crystal structure shows not only that atom Oδ2 of Asp199 (equivalent to Asn614′ in *A. vinelandii* E2p) is 3.4 Å apart from atom Nδ1 of His195 (Figure 4d), making exactly the same interaction

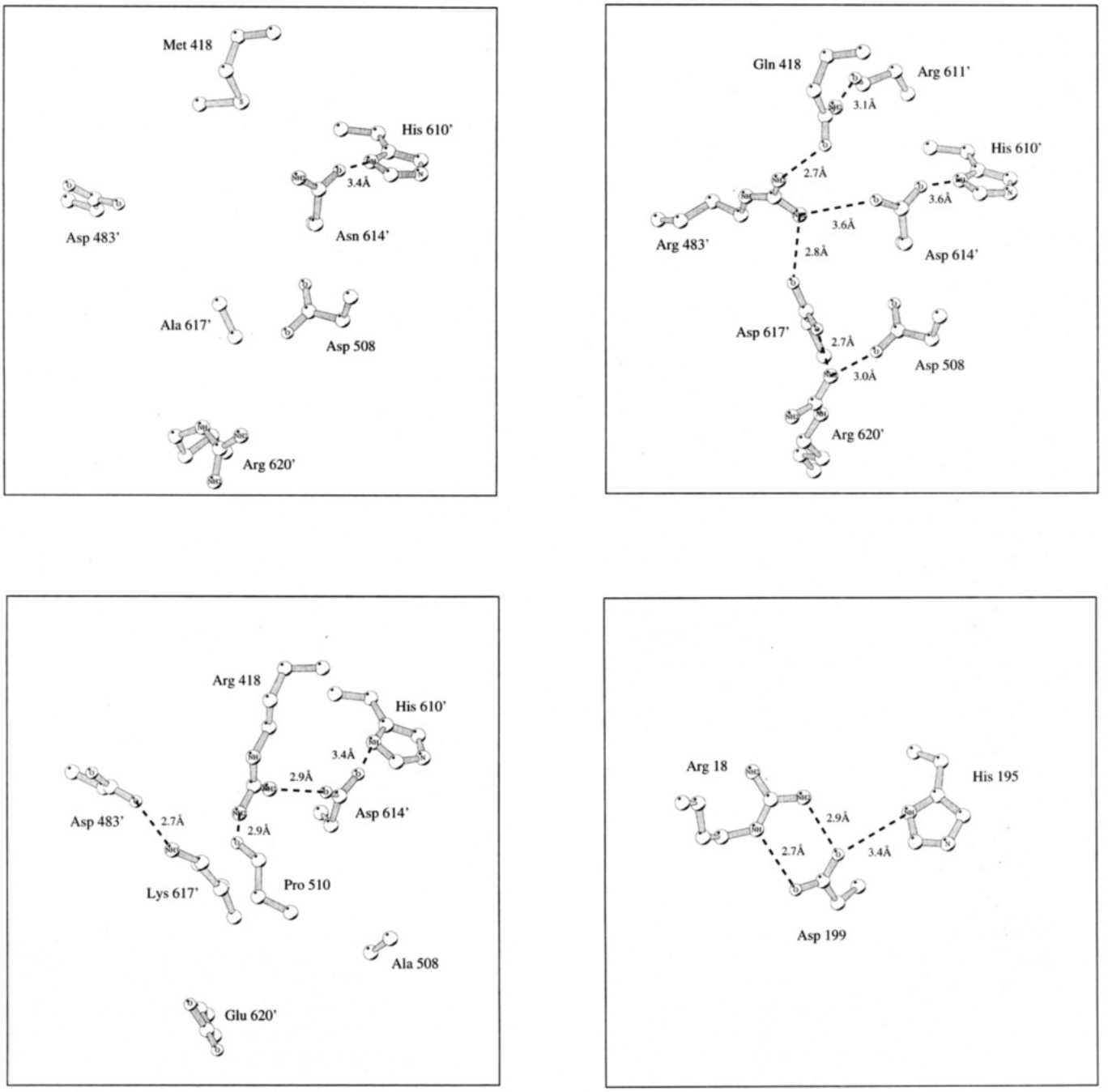

FIGURE 4: Hydrogen bond network in the active site of (a, top left panel) the liganded form of *A. vinelandii* E2p (Mattevi et al., 1993c), (b, top right panel) an active site model of *E. coli* E2p, (c, bottom left panel) an active site model of yeast E2p, and (d, bottom right panel) chloramphenicol acetyltransferase (Leslie, 1990). The drawings were prepared with Molscript (Kraulis, 1991) using dashed lines for the presentation of hydrogen bonds. The hydrogen bond distances are given in angstroms. For reasons of simplicity and comparability, the residue numbers of *A. vinelandii* E2p are used for the *E. coli* and yeast models.

as Asn614′ does in the liganded wild-type *A. vinelandii* E2p structure, but also that atoms Oδ1 and Oδ2 of Asp199 are engaged in hydrogen bonds with Nϵ and Nη2 of Arg18, forming hydrogen bonds of 2.9 and 2.7 Å, respectively (Leslie, 1990). A mutation of Arg18 in chloramphenicol acetyltransferase into a valine residue illustrates the importance of the arginine residue at position 18: the k_{cat} is decreased by a factor of 9 with a slightly increased K_M value for the substrates chloramphenicol and CoA (Lewendon et al., 1988). Clearly, the salt bridge partner of Asp199 in CAT is affecting the catalytic efficiency of CAT.

In order to evaluate the situation in the E2p family, models of the active site of *E. coli* and yeast E2p were built on the basis of the active site structure of *A. vinelandii* E2p (Mattevi et al., 1993c). All protein residues within a sphere of 8 Å around Asn614′ of the *A. vinelandii* enzyme were changed according to the sequence alignment given in Table 4. The side chain orientations of His610′, Asn/Asp614′, and Asp508 were left unaltered, and the remaining side chains were adjusted in order to maximize the number of hydrogen bonds. Both the *E. coli* and the yeast active site models so obtained displayed an extensive hydrogen bonding network between charged residues (Figure 4b,c). Most significantly perhaps, in both the yeast and the *E. coli* active site models a side chain conformer of an arginine residue corresponding, respectively, to positions Asp483′ and Met418 in the *A. vinelandii* enzyme can be easily accommodated to form a hydrogen bond with the active site aspartate (hydrogen bonds

Table 4: Alignment of Protein Sequences from Dihydrolipoamide Acetyltransferases (E2p)

	residue									
enzyme source	418	425	435′	483′–484′	507–509	512–513	560	608′	610′–617′	620′
E2p, *A. vi*[b]	M	L	V	**DF**	**VDT**	GL	L	Y	**HRVINGAA**	**R**
E2p, *E. coli*[c]	Q	L	V	**RF**	VDT	GL	I	F	**HRVIDGAD**	**R**
E2p, yeast[d]	**R**	L	Y	**DA**	VAT	GL	M	F	**HRTIDGAK**	**E**

[a] Residues within a sphere of 8 Å around Asn614′ only are listed. Charged residues are indicated in boldface letters. For reasons of simplicity, the residue numbers of the dihydrolipoamide acetyltransferases from *A. vinelandii* only are displayed. [b] Hanemaaijer et al. (1988). [c] Stephens et al. (1983). [d] Niu et al. (1988).

listed in Figure 4a–d). We postulate, therefore, that these Asp–Arg salt bridges occur in the yeast and *E. coli* enzymes, thereby resembling the Asp–Arg salt bridge in chloramphenicol acetyltransferase.

The decrease in activity after changing the His-Asp-Arg triad into His-Asn-Arg in *E. coli* and yeast E2p as well as in chloramphenicol acetyltransferase is likely to be due to the fact that the Nδ2 atom of the asparagine side chain cannot make the favorable hydrogen bond with the NH functions of the guanidinium group of the arginine residue which the Oδ2 was able to make. As a consequence, the asparagine might remain too far away from the histidine, or the histidine moves too far from its optimal position, or a combination of these effects. This reflects the precision required for the optimal position of the catalytic residues in the center of the active site channel of these acetyltransferases.

Therefore, it seems that the His-Asp-Arg triad in yeast E2p, *E. coli* E2p, and chloramphenicol acetyltransferase is one possibility for ensuring optimal activation of the general catalytic base histidine, while the His-Asn pair in the *A. vinelandii* enzyme achieves a very similar result. The function of the arginine residue in the triads is likely a moderation of the enhancement of the aspartate on the nucleophilicity of the histidine. In the case where the arginine is absent, as in the *A. vinelandii* N614D mutant, the aspartate moiety effects the imidazole ring of His610′ in a suboptimal way, and an asparagine ensures better catalysis. If our hypothesis would prove to be correct, then certain double mutants of *A. vinelandii* E2p should have better activity than the N614D mutant. Specifically, introduction of an arginine side chain at position 483′ or 418 should lead to the formation of His-Asp-Arg triads. The corresponding double mutants D483R/N614D and M418R/N614D should mimic the active sites of the *E. coli* and yeast enzymes, respectively, and should approach the activity of the *A. vinelandii* wild-type enzyme.

CONCLUSION

The three-dimensional structure of three active site mutants of E2pCD has revealed that the decrease in enzymatic activity of these mutants is not due to large conformational rearrangements of the enzyme, but due to the absence of three essential side chains. In the *A. vinelandii* enzyme, Ser558 is likely to be involved in transition state stabilization and His610′ in proton abstraction, functions which are analogous to those proposed for Ser148 and His195 in chloramphenicol acetyltransferase (Kleanthous et al., 1985; Lewendon et al., 1990). Analysis of the structures also provides evidence for the role of residue 614′ (*A. vinelandii* numbering) in catalysis. In one class of acetyltransferases, a His-Asp-Arg triad provides optimal activity; in a second class, a His-Asn pair provides the same efficiency. The asparagine and aspartate residues may act as "histidine activators" while in the "triad class" of acetyl transferases an arginine modulates the activator aspartate. Ser558 is likely to be involved in transition state stabilization and His610′ in proton abstraction.

ACKNOWLEDGMENT

We thank Galya Obmolova for excellent assistance in crystal growth and Stewart Turley for his assistance with data collection.

REFERENCES

Ausubel, F. M., Brent, R., Kingston, R. E., Moore, D. D., Seidman, J. G., Smith, J. A., & Struhl, K. (1987) In *Current protocols in molecular biology*, John Wiley & Sons, New York.

Bresters, T. W., de Abreu, R. A., de Kok, A., Visser, J., & Veeger, C. (1975) *Eur. J. Biochem. 59*, 335–345.

Brünger, A. T. (1990) in *X-PLOR Manual Version 2.1*, Yale University, New Haven, CT.

CCP4 (1986) in *The SERC (UK) Collaborative Computing Project No. 4, a suite of programs for protein crystallography, CCP4 Program Suite*, Daresbury Laboratory.

Dardel, F., Laue, E., & Perham, R. N. (1991) *Eur. J. Biochem. 201*, 203–209.

Gibson, T. J. (1984) Ph.D. Thesis, University of Cambridge.

Gregoret, L. M., Rader, S. D., Fletterick, R. J., & Cohen, F. E. (1991) *Proteins: Struct., Funct., Genet. 9*, 99–107.

Griffin, T. A., & Chuang, D. T. (1990) *J. Biol. Chem. 265*, 13174–13180.

Guest, J. R. (1987) *FEMS Microbiol. Lett. 44*, 417–422.

Guest, J. R., Ali, S. T., Artymiuk, P., Ford, G. C., Green, J., & Russell, G. C. (1990) in *Biochemistry and Physiology of thiamin diphosphate enzymes* (Bisswanger, H., & Ullrich, J., Eds.) pp 176–183, Verlag Chemie, Weinheim.

Hanemaaijer, R., Janssen, A., de Kok, A., & Veeger, C. (1988) *Eur. J. Biochem. 174*, 593–599.

Howard, A. J., Gilliland, G. L., Finzel, B. C., & Poulos, T. L. (1987) *J. Appl. Crystallogr. 20*, 383–387.

Jones, T. A., Zou, J.-Y., & Cowan, S. W. (1991) *Acta Crystallogr. A47*, 110–119.

Kleanthous, C., Cullis, P. M., & Shaw, W. V. (1985) *Biochemistry 24*, 5307–5313.

Kraulis, P. J. (1991) *J. Appl. Crystallogr. 24*, 946–950.

Kunkel, T. A., Roberts, J. D., & Zakour, R. A. (1987) *Methods Enzymol. 154*, 367–382.

Leslie, A. G. W. (1990) *J. Mol. Biol. 213*, 167–186.

Lewendon, A., Murray, I. A., Kleanthous, C., Cullis, P. M., & Shaw, W. V. (1988) *Biochemistry 27*, 7385–7390.

Lewendon, A., Murray, I. A., Shaw, W. V., Gibbs, M. R., & Leslie, A. G. W. (1990) *Biochemistry 29*, 2075–2080.

Machin, P. A., Wonacott, A. J., & Moss, D. (1983) *Daresbury Lab. News 10*, 3–9.

Mattevi, A., Schierbeck, A. J., & Hol, W. G. J. (1991) *J. Mol. Biol. 220*, 975–994.

Mattevi, A., Obmolova, G., Sokatch, J. R., Betzel, C., & Hol, W. G. J. (1992a) *Proteins: Struct., Funct., Genet. 13*, 336–351.

Mattevi, A., Obmolova, G., Schulze, E., Kalk, K. H., Westphal, A. H., de Kok, A., & Hol, W. G. J. (1992b) *Science 255*, 1544–1550.

Mattevi, A., Obmolova, G., Kalk, K. H., Berkel, W. J., & van Hol, W. G. J. (1993a) *J. Mol. Biol. 230*, 1200–1215.

Mattevi, A., Obmolova, G., Kalk, K. H., Westphal, A. H., de Kok, A., & Hol, W. G. J. (1993b) *J. Mol. Biol. 230*, 1183−1199.
Mattevi, A., Obmolova, G., Kalk, K. H., Teplyakov, A., & Hol, W. G. J. (1993c) *Biochemistry 32*, 3887−3901.
Niu, X.-D., Browning, K. S., Behal, R. H., & Reed, L. J. (1988) *Proc. Natl. Acad. Sci. U.S.A. 85*, 7546−7550.
Niu, X.-D., Stoops, J. K., & Reed, L. J. (1990) *Biochemistry 29*, 8614−8619.
Perham, R. N. (1991) *Biochemistry 30*, 8501−8512.
Perham, R. N., Duckworth, H. W., & Roberts, G. C. K. (1981) *Nature 292*, 474−477.
Ramachandran, G. N., Venkatachalam, C. M., & Krimm, S. (1966) *Biophys. J. 6*, 849−872.
Read, R. J. (1986) *Acta Crystallogr. A42*, 140−149.
Reed, L. J. (1974) *Acc. Chem. Res. 7*, 40−46.
Reed, L. J., & Hackert, M. L. (1990) *J. Biol. Chem. 265*, 8971−8974.
Reed, L. J., Koike, M., Levitch, M. E., & Leach, F. R. (1958) *J. Biol. Chem. 232*, 143−158.
Robien, M. A., Clore, G. M., Omichinski, J. G., Perham, R. N., Appella, E., Sakaguchi, K., & Gronenborn, A. M. (1992) *Biochemistry 31*, 3463−3471.
Russell, G. C., & Guest, J. R. (1990) *Biochem. J. 269*, 443−450.
Russell, G. C., & Guest, J. R. (1991a) *Biochim. Biophys. Acta 1076*, 225−232.
Russell, G. C., & Guest, J. R. (1991b) *Proc. R. Soc. London (Biol.) 243*, 155−160.
Sanger, F., Nicklen, S., & Coulson, A. R. (1977) *Proc. Natl. Acad. Sci. U.S.A. 74*, 5463−5467.
Sato, M., Yamamoto, M., Imada, K., & Katsube, Y. J. (1992) *Appl. Crystallogr. 25*, 348−357.
Schulze, E., Westphal, A. H., Obmolova, G., Mattevi, A., Hol, W. G. J., & de Kok, A. (1991a) *Eur. J. Biochem. 201*, 561−568.
Schulze, E., Benen, J. A. E., Westphal, A. H., & de Kok, A. (1991b) *Eur. J. Biochem. 200*, 29−34.
Stephens, P. E., Darlison, M. G., Lewis, H. M., & Guest, J. R. (1983) *Eur. J. Biochem. 133*, 481−489.
Thaller, C., Weaver, L. H., Eichele, G., Wilson, E., Karlsson, R., & Jansonius, J. N. (1981) *J. Mol. Biol. 147*, 465−469.

BI942110M